

Fault-tolerant quantum computation in concatenation of verified cluster states

Keisuke Fujii and Katsuji Yamamoto

Department of Nuclear Engineering, Kyoto University, Kyoto 606-8501, Japan

(Dated: November 27, 2018)

A novel scheme is presented for fault-tolerant quantum computation based on the cluster model. Some relevant logical cluster states are constructed in concatenation by post-selection through verification, without necessity of recovery operation, where a suitable code such as the Steane's 7-qubit code is adopted for transversal operations. This simple concatenated construction of verified cluster states achieves a high noise threshold $\sim 1\%$, and restrains the divergence of resources.

PACS numbers: 03.67.Lx, 03.67.Pp, 03.67.-a

In order to implement reliable computation in physical systems, the problem of noise should be overcome. Then, fault-tolerant quantum computation with error correction has been investigated [1, 2, 3, 4, 5, 6, 7]. In the usual quantum error correction (QEC), error syndromes are detected on encoded qubits, and the errors are corrected according to them. The noise thresholds for fault-tolerant computation are calculated to be about $10^{-6} - 10^{-3}$ depending on the QEC protocols and noise models [6, 7, 8, 9, 10, 11, 12, 13, 14, 15]. A main motivation for QEC comes from the fact that in the circuit model the original qubits should be used throughout computation even if errors occur on them.

On the other hand, more robust computation may be performed in measurement-based quantum computers [16, 17, 18, 19, 20, 21, 22]. Teleportation from old qubits to fresh ones is made by measurements for gate operations, and the original qubits are not retained. An interesting computation model with error-correcting teleportation is proposed based on encoded Bell pair preparation and Bell measurement, which provides high noise thresholds $\sim 1 - 3\%$ [21, 22]. The cluster model or one-way computer [18] should also be considered for fault-tolerant computation. A highly entangled state, called a cluster state, is prepared, and gate operations are implemented by measuring the qubits in the cluster with feedforward for the post-selection of measurement bases. This gate operation in the cluster model may be viewed as the one-bit teleportation [17]. A promising scheme for linear optical quantum computation is proposed, where deterministic gates are implemented by means of the cluster model [23]. Fault-tolerant computation is built up for this optical scheme by using a clustered version of the syndrome extraction for QEC [6]. The noise thresholds are estimated to be about 10^{-3} for photon loss and 10^{-4} for depolarization [24]. The threshold result is also argued by simulating the QEC circuits with clusters [25, 26, 27]. Some direct approaches are, on the other hand, considered for the fault-tolerant one-way computation [28, 29].

In this Letter, we present a novel scheme of fault-tolerant quantum computation by making a better use of the unique feature of the cluster model. Specifically, the fault-tolerant computation is implemented by *concatenated construction and verification of logical cluster states via one-way computation with post-selection*. A

number of cluster states are constructed in parallel with error detection, and the unsuccessful ones are discarded, selecting clean cluster states. The high-fidelity preparation of Bell state (or its cluster version) is adopted for the error-correcting teleportation [21, 22, 29]. It is also considered that improved ancilla preparation increases the noise threshold [30, 31]. In the present scheme, even gate operations as cluster states are prepared and verified by post-selected computing to reduce errors more efficiently. That is, gate operations are *pre-selected*, or errors are corrected before the computation starts, say *error pre-correction*, which is enabled by means of the cluster model where the order of operations can be changed suitably (see Ref. [28] for an early idea). This is quite distinct from the standard QEC, where errors are corrected after noisy operations, even via teleportation.

While high-fidelity state preparation is achieved by post-selection, huge resources are generally required due to the exponentially diminishing net success probability according to the computation size, which is a serious obstacle for scalability [21, 22, 28, 29]. We here succeed to overcome this dilemma in post-selection by presenting a systematic method of concatenation to construct logical cluster states through verification. As described in the following, the necessary post-selections are minimized and localized, which enables off-line gate operations prior to the computation, as verified logical clusters. This provides the scalable concatenation of post-selection in the cluster model. Then, a high noise threshold $\sim 1\%$ is achieved by post-selection, while the resources usage is moderate, being comparable with or even less than the circuit-based QEC schemes. This concatenated cluster construction is implemented suitably by adopting a class of stabilizer codes of Calderbank-Shor-Steane, e.g., the Steane's 7-qubit code [2, 3, 14]. The logical measurements of Pauli operators as well as the Clifford gates, H , S and $C-Z$, are implemented transversally on such a quantum code. The non-Clifford $\pi/8$ gate is even operated for universal computation by preparing a specific qubit and making a transversal measurement [28, 29].

(i) *Fundamental clusters*: A set of gate operations in one-way computation may be decomposed into some fundamental clusters. This decomposition enables us to post-select the computation without divergence of resources in concatenation. The fundamental clusters are

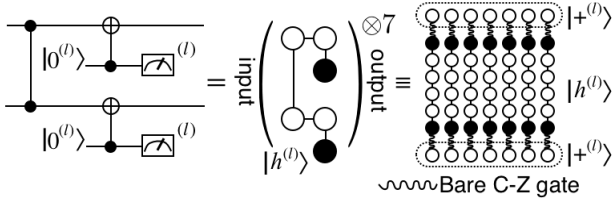


FIG. 1: C-Z gate with single verification at the level l . Each $|+\rangle^{(l)}$ ($= H|0\rangle^{(l)}$) is encoded through an H rotation to the level- $(l-1)$ \bullet qubits in $|h\rangle^{(l)}$'s with bare C-Z gates.

specifically taken as $|h\rangle^{(l)}$, $|0\rangle^{(l)}$, $|+\rangle^{(l)}$ at the logical level l ($l \geq 1$), which are composed of level- $(l-1)$ qubits. The code states $|0\rangle^{(l)}$ and $|+\rangle^{(l)}$ are used as ancillas for encoding and syndrome detection. The hexa-cluster $|h\rangle^{(l)}$, as a linear cluster of 6 qubits, represents an elementary unit of gate operations. These fundamental clusters are combined by *bare* C-Z gates (transversal concatenation of physical C-Z gates without verification) to implement one-way computations such as C-Z gates with syndrome detections and the concatenated construction of logical clusters through verification, $\{|h\rangle^{(l)}, |0\rangle^{(l)}, |+\rangle^{(l)}\} \rightarrow \{|h\rangle^{(l+1)}, |0\rangle^{(l+1)}, |+\rangle^{(l+1)}\}$.

(ii) *Verified C-Z gates*: A C-Z gate with single verification at the level- l is implemented by combining $7|h\rangle^{(l)}$'s and $2|+\rangle^{(l)}$'s, as shown in the right cluster diagram of Fig. 1. This combination of clusters is schematically denoted by the symbol “ $\otimes 7$ ” (henceforth used conveniently), which does not simply imply the tensor product but also includes the encoding of ancilla code blocks (marked with \bullet). The level- $(l-1)$ \bullet qubit in each $|h\rangle^{(l)}$ is connected through an H rotation to the corresponding level- $(l-1)$ qubit in an ancilla $|+\rangle^{(l)}$ with a bare C-Z gate (wavy line); $|+\rangle^{(l)} = H|0\rangle^{(l)}$ is teleported as $|0\rangle^{(l)}$. The 2 input level- l code blocks are similarly encoded via teleportation to the 2×7 level- $(l-1)$ \circ qubits (see also \oplus 's in Fig. 3). As seen from the circuit equivalent in Fig. 1, the error syndromes of the 2 level- l qubits through the C-Z gate are extracted for verification [6, 7, 8]. A C-Z gate with double verification is also implemented by combining $7 \times 3|h\rangle^{(l)}$'s and $8|+\rangle^{(l)}$'s in Fig. 2 (the ancillas are encoded to the \bullet qubits). Here, the errors in the ancilla $|+\rangle^{(l)}$'s ($|0\rangle^{(l)}$'s via teleportation) are even detected for higher fidelity. It should be remarked that at the beginning of concatenation the verified level-1 C-Z gates may be implemented efficiently by means of the circuit diagrams in Figs. 1 and 2, without using $|h\rangle^{(1)}$'s. This is because $|h\rangle^{(1)}$'s, as chains of physical qubits without verification, are somewhat noisy.

(iii) *Concatenated cluster construction*: The level- $(l+1)$ hexa-cluster $|h\rangle^{(l+1)}$ is constructed in Fig. 3 by combining the level- l clusters $|h\rangle^{(l)}$, $|0\rangle^{(l)}$, $|+\rangle^{(l)}$ with bare C-Z gates. Here, it is understood that the 7 level- $(l-1)$ \oplus qubits in a transversal set of 7 $|h\rangle^{(l)}$'s are connected to a $|0\rangle^{(l)}$ (not shown explicitly) with bare C-Z gates to encode $|+\rangle^{(l)} = H|0\rangle^{(l)}$ via teleportation, as done

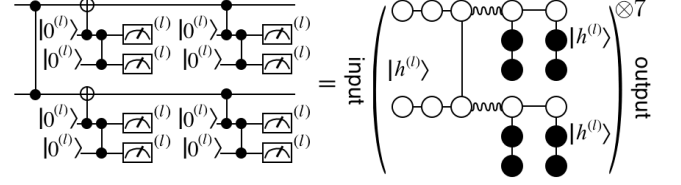


FIG. 2: C-Z gate with double verification at the level l . Ancilla $|+\rangle^{(l)}$'s should be encoded to the \bullet qubits as Fig. 1.

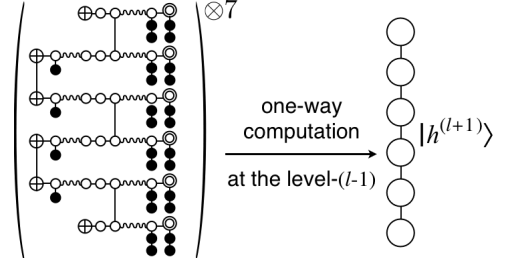


FIG. 3: Concatenated construction of hexa-cluster.

similarly for the \bullet qubits in Fig. 1. The $6|+\rangle^{(l)}$'s encoded to the $6 \times 7 \oplus$ qubits are entangled through 2 C-Z gates with single verification (Fig. 1) and 3 C-Z gates with double verification (Fig. 2) to form the $|h\rangle^{(l+1)}$ via one-way computation. These C-Z gates are combined in such ways that each qubit has at most one bare C-Z connection (wavy line), and that the output qubits (\odot) as $|h\rangle^{(l+1)}$ are doubly verified. The level- $(l-1)$ qubits, except \odot 's, are measured to implement the computation. In this transversal level- $(l-1)$ computation, the level- l syndromes can be extracted by the measurements of the level- $(l-1)$ \bullet qubits. Then, if all the level- l syndromes are correct, the 6×7 level- $(l-1)$ \odot qubits survive as the verified $|h\rangle^{(l+1)}$ passing the post-selection. (Once an error syndrome is detected, the computation is abandoned, among many parallel constructions.) That is, the level- l gate operation to be implemented with $|h\rangle^{(l+1)}$ has been verified beforehand by these level- l syndrome extractions. As noted previously, the level-2 construction may be implemented efficiently with the circuit diagrams in Figs. 1 and 2 for the verified level-1 C-Z gates.

The level-1 $|0\rangle^{(1)}$ and $|+\rangle^{(1)}$ are prepared through verification by the stabilizer measurement and syndrome extraction with the usual method [6, 7, 8]. Then, the level- $(l+1)$ $|+\rangle^{(l+1)}$ and $|0\rangle^{(l+1)}$ are encoded with the level- l fundamental clusters via one-way computation in cluster diagrams, such as Fig. 3 for the $|h\rangle^{(l+1)}$, which include suitably the verified C-Z gates (Figs. 1 and 2).

(iv) *Universal computation*: The fundamental clusters are constructed through verification up to the highest logical level \bar{l} to achieve the fidelity required for a given computation size. Then, the desired computation is implemented by combining the highest-level hexa-clusters $|h\rangle^{(\bar{l}+1)}$ with bare C-Z gates. The preparation of $|\pi/8\rangle^{(\bar{l})} = \cos(\pi/8)|0\rangle^{(\bar{l})} + \sin(\pi/8)|1\rangle^{(\bar{l})}$ is also needed

for universal computation to operate the non-Clifford $\pi/8$ gate $e^{-i(\pi/8)Z}$ by transversal measurement on the 7-qubit code [28, 29]. The level-1 $|\pi/8^{(1)}\rangle$ is encoded by the usual method [12]. Then, the upper-level $|\pi/8^{(l)}\rangle$ is encoded with the lower-level $|\pi/8^{(l-1)}\rangle$, similarly to the other fundamental clusters. The logical failure of $|5\pi/8^{(l)}\rangle$ cannot be detected in encoding the $|\pi/8^{(l)}\rangle$, because it has also the correct syndrome. This small mixture of $|5\pi/8^{(l)}\rangle$ is hence not reduced by the concatenation, though the constructed $|\pi/8^{(l)}\rangle$ is kept on the code space by the verification, retaining the logical fidelity as the $|\pi/8^{(1)}\rangle$. This slightly noisy $|\pi/8^{(l)}\rangle$ is even useful to obtain the desired high fidelity $|\pi/8^{(l)}\rangle$ at the highest level by using the magic state distillation with Clifford operations [32].

The errors on the qubits and Pauli frames should be considered properly to estimate the measurement errors and noise threshold in the one-way computation with post-selection to prepare clean logical clusters.

(i) *Homogeneous errors on qubits:* The level-2 fundamental clusters are first constructed, and their constituent level-1 qubits are doubly verified. Then, it is reasonably expected that the level-0 qubits (as marked with \odot in Fig. 3) encoded in these verified level-1 qubits contain independently and identically distributed (homogeneous) depolarization errors in the leading order [31]. The homogeneous error probabilities ϵ_A ($A = X, Y, Z$) of these level-0 qubits are determined essentially by the error probabilities p_{AB} of the physical gates which are used transversally for the level-1 double verification; $\epsilon_X = p_{XI}$, $\epsilon_Y = p_{YI}$, $\epsilon_Z = 2p_{ZI}$ from the circuit diagram in Fig. 2. (The errors on the input qubits are almost eliminated through the verification.) In the level- $(l+1)$ construction, as described in Fig. 3, *any operations are not implemented directly on the output level- l qubits, which are composed of the level- $(l-1)$ \odot qubits, but the entanglement by the verified C-Z gates is transferred to prepare the verified level- $(l+1)$ clusters via teleportation (one-way computation) of the level- $(l-1)$ qubits.* Hence, these output level- l qubits inherit transversally the homogeneous errors ϵ_A of the constituent level-0 qubits after the level-1 verification. The prepared level- $(l+1)$ clusters are further used for the level- $(l+2)$ construction, and some pairs of level- l qubits in these clusters are connected by bare C-Z gates. Then, extra errors are added to the constituent level-0 qubits through the bare C-Z gate as $\epsilon'_X = \epsilon_X + p_{XB}$, $\epsilon'_Y = \epsilon_Y + p_{YB}$, $\epsilon'_Z = \epsilon_Z + \epsilon_X + \epsilon_Y + p_{ZB}$ (summed over $B = I, X, Y, Z$).

(ii) *Errors in measurements and threshold:* By the measurements of level- $(l-1)$ qubits to construct the level- $(l+1)$ clusters, as in Fig. 3, the level- $(l-1)$ Pauli frames of the neighboring qubits are updated. The output level- l qubits to form the level- $(l+1)$ clusters are, however, doubly verified, and hence the propagation of the preceding measurement errors is prohibited by post-selection as the Pauli frame errors of the constituent level- $(l-1)$ \odot qubits. The fundamental clusters are therefore prepared

to be free from the Pauli frame errors (up to the higher orders) through the concatenation. In the absence of Pauli frame errors at the level- $(l-1)$ and below, the error probability $p_q^{(l)}$ to measure solely a level- l qubit contained in a verified level- $(l+1)$ cluster is reduced transversally to the level-0 $p_q^{(0)}$ on the 7-qubit code with distance 3 as

$$p_q^{(l)} \simeq \tau C_2 (p_q^{(l-1)})^2 \simeq (\tau C_2 p_q^{(0)})^{2^l} / \tau C_2. \quad (1)$$

The level- l qubit is actually measured during the upper level- $(l+2)$ cluster construction. Then, the measurement error of this qubit becomes some multiple of $p_q^{(l)}$, including its level- l Pauli frame error due to the propagation of the preceding measurement errors.

The level-0 qubits with the homogeneous errors ϵ'_A through bare C-Z connection ($\epsilon_A < \epsilon'_A$) are measured in the X basis with the error probability $p_q^{(0)} = \epsilon'_Z + \epsilon'_Y + p_M$ (p_M is the error probability of physical measurement). Then, the noise threshold is given from Eq. (1) as

$$p_q^{(0)} = D p_e < 1/\tau C_2 \rightarrow p_{\text{th}} = (\tau C_2 D)^{-1}, \quad (2)$$

where p_e represents the mean error probability of physical operations ($D \sim 1$). It is estimated as $p_{\text{th}} = 0.042$ ($D = 17/15$) typically with $p_{AB} = (1/15)p_e$ for ϵ'_A and $p_M = (4/15)p_e$ [22]. We have made a numerical simulation to confirm the above estimates concerning the errors on the qubits and Pauli frames in the concatenation. The Pauli frame errors are really absent in the successful logical clusters in the leading order, as considered in Eq. (1).

The physical resources (qubits and gates) are calculated by counting the numbers of hexa-clusters, ancilla qubits and bare C-Z gates in the diagrams such as Figs. 1, 2, 3. (The details will be presented in a forthcoming paper.) They are given as the recurrence relations for the C-Z gates with single (S) and double (D) verifications, and the fundamental clusters $|\alpha\rangle = |h\rangle, |0\rangle, |+\rangle$:

$$R_S^{(l)} = 7R_h^{(l)} + 2(R_+^{(l)} + R_b^{(l)})(l \geq 2), \quad (3)$$

$$R_D^{(l)} = 3 \times 7R_h^{(l)} + 8(R_+^{(l)} + R_b^{(l)}) + 2R_b^{(l)}(l \geq 2), \quad (4)$$

$$R_\alpha^{(l+1)} = \sum_{O=S,D,0,b} n_\alpha^O R_O^{(l)} / p_\alpha^{(l+1)}(l \geq 1), \quad (5)$$

where $R_b^{(l)} = 7^l$ for a bare C-Z gate, $(n_\alpha^S, n_\alpha^D, n_\alpha^0, n_\alpha^b) = (2, 3, 6, 4)_h, (6, 7, 11, 15)_0, (5, 6, 10, 14)_+$, and the success probabilities $p_\alpha^{(l+1)}$ for the cluster verification are included. The level-1 resources are given by $R_0^{(1)} = 69/p_0^{(1)}$, $R_+^{(1)} = 72/p_+^{(1)}$, $R_S^{(1)} = 3 \times 7 + 2R_0^{(1)}$, $R_D^{(1)} = 9 \times 7 + 8R_0^{(1)}$ [$n_\alpha^0 R_0^{(1)} \rightarrow n_\alpha^0 R_+^{(1)}$ for $l = 1$ in Eq. (5)], based on the circuit diagrams in Figs. 1 and 2 with physical C-Not and C-Z gates. Somewhat more resources are used if the cluster computation is made even at the level-0, by substituting C-Not \rightarrow C-HZH.

The success probabilities $p_\alpha^{(l+1)}$ are evaluated by the numerical simulation, which actually approach unity at the level-3 or higher as the logical measurement error $p_q^{(l)}$

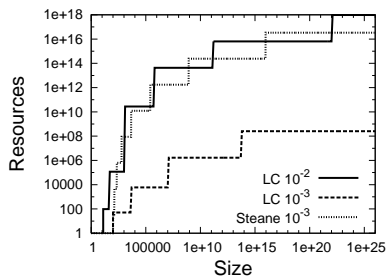


FIG. 4: Resources for the present scheme of verified logical clusters (LC) with $p_e = 10^{-2}$ and 10^{-3} , which are compared with the Steane's QEC scheme with $p_e = 10^{-3}$.

is reduced rapidly below the threshold. The resources are estimated in the above relations with these $p_\alpha^{(l+1)}$, depending on the computation size N with the highest level $\bar{l} \sim \log_2(\log_{10} N)$ to achieve the accuracy $0.1/N$. The results for $R_0^{(l)}$ ($> R_{h,+}^{(l)}$) are shown in Fig. 4 for the present scheme of verified logical clusters (LC) with $p_e = 10^{-2}$ and 10^{-3} , which are compared with the circuit-based Steane's QEC scheme with $p_e = 10^{-3}$ [9]. Each step in these graphs means the up of logical level by one. The present scheme really consumes much less resources than the Steane's QEC scheme for $p_e \leq 10^{-3}$.

We also find that compared with the C_4/C_6 scheme with post-selection (or with error-correction) [21], the present scheme provides a comparable threshold, requiring much less (or comparable) resources. Furthermore,

the present scheme has a lot of room for improvement. The Fibonacci scheme such as C_4/C_6 based on the 4-qubit error-detecting code may be applied to improve especially the resources. The optimal decoding (adaptive concatenation) [33] is readily available to boost the noise threshold up to 9% with reasonable resources.

The memory errors may be significant in this post-selection scheme without recovery operation. The qubits to form the clusters are not touched directly (but via one-bit teleportation) through the verified construction after the level-1 verification. Then, the memory errors accumulate until they are measured in the upper-level construction. The memory errors are added as $p_q^{(0)} + \bar{l}(n\tau_m p_e)$, where $\tau_m p_e$ denotes the probability of memory error with the effective waiting time τ_m for one measurement, and n is the number of waiting time steps at each concatenation level (e.g., $n = 12$ for the hexa-cluster). The noise threshold is hence determined as $p_{th} \sim [\tau C_2 \{1 + \log_2(\log_{10} N)n\tau_m\}]^{-1}$, depending on the computation size N with the highest level $\bar{l} \sim \log_2(\log_{10} N)$. For example, $p_{th} \sim 1\%$ for $N \sim 10^{20}$ and $\tau_m = 0.1$ ($n \sim 10$), which will be tolerable for practical computations. In order to overcome essentially the memory error accumulation, the fundamental clusters as two-colorable graph states may be refreshed at each level by using a purification protocol [34].

This work was supported by International Communications Foundation (ICF).

-
- [1] P. W. Shor, Phys. Rev. A **52**, R2493 (1995).
[2] A. R. Calderbank and P. W. Shor, Phys. Rev. A **54**, 1098 (1996).
[3] A. M. Steane, Phys. Rev. Lett. **77**, 793 (1996).
[4] P. W. Shor, *Proceedings of the 37th Annual Symposium on Foundations of Computer Science* (IEEE Computer Society Press, Los Alamitos, CA, 1996), p. 56.
[5] D. P. DiVincenzo and P. W. Shor, Phys. Rev. Lett. **77**, 3260 (1996).
[6] A. M. Steane, Phys. Rev. Lett. **78**, 2252 (1997).
[7] A. M. Steane, Fortschr. Phys. **46**, 443 (1998).
[8] A. M. Steane, Nature **399**, 124 (1999).
[9] A. M. Steane, Phys. Rev. A **68**, 042322 (2003).
[10] A. Yu. Kitaev, Russ. Math. Surv. **52**, 1191 (1997).
[11] J. Preskill, Proc. R. Soc. London A **454**, 385 (1998).
[12] E. Knill, R. Laflamme, and W. H. Zurek, Proc. R. Soc. London A **454**, 365 (1998); Science **279**, 342 (1998).
[13] D. Gottesman, Ph.D. thesis, California Institute of Technology (1997).
[14] D. Gottesman, Phys. Rev. A **57**, 127 (1998).
[15] D. Aharonov and M. Ben-Or, *Proceedings of the 29th Annual ACM Symposium on the Theory of Computation* (ACM Press, New York, 1998), p. 176.
[16] D. Gottesman and I. L. Chuang, Nature **402**, 390 (1999).
[17] X. Zhou, D. W. Leung, and I. L. Chuang, Phys. Rev. A **62**, 052316 (2000).
[18] R. Raussendorf and H. J. Briegel, Phys. Rev. Lett. **86**, 5188 (2001); R. Raussendorf, D. E. Browne, and H. J. Briegel, Phys. Rev. A **68**, 022312 (2003).
[19] M. A. Nielsen, Phys. Lett. A **308**, 96 (2003).
[20] R. Prevedel, M. S. Tame, A. Stefanov, M. Paternostro, M. S. Kim, and A. Zeilinger, Phys. Rev. Lett. **99**, 250503 (2007).
[21] E. Knill, Nature **434**, 39 (2005).
[22] E. Knill, Phys. Rev. A **71**, 042322 (2005).
[23] M. A. Nielsen, Phys. Rev. Lett. **93**, 040503 (2004).
[24] C. M. Dawson, H. L. Haselgrove, and M. A. Nielsen, Phys. Rev. Lett. **96**, 020501 (2006); Phys. Rev. A **73**, 052306 (2006).
[25] R. Raussendorf, Ph.D. thesis, Ludwig-Maximilians Universität München (2003).
[26] M. A. Nielsen and C. M. Dawson, Phys. Rev. A **71**, 042323 (2005).
[27] P. Aliferis and D. W. Leung, Phys. Rev. A **73**, 032308 (2006).
[28] K. Fujii and K. Yamamoto, quant-ph/0611160 (2006).
[29] M. Silva, V. Danos, E. Kashefi, and H. Ollivier, New J. Phys. **9**, 192 (2007).
[30] B. W. Reichardt, quant-ph/0406025 (2004).
[31] B. Eastin, Phys. Rev. A **75**, 022301 (2007).
[32] S. Bravyi and A. Kitaev, Phys. Rev. A **71**, 022316 (2005).
[33] D. Poulin, Phys. Rev. A **74**, 052333 (2006); J. Fern, Phys. Rev. A **77**, 010301(R) (2008).
[34] W. Dür, H. Aschauer, and H. J. Briegel, Phys. Rev.

Lett. **91**, 107903 (2003); H. Aschauer, W. Dür, and H. J. Briegel, Phys. Rev. A **71**, 012319 (2005).